



Photoinduced spin crossover in a Fe-picolylamine complex: A far-infrared study on single crystals

Okamura, Hidekazu ; Matsubara, M. ; Nanba, Takao ; Tayagaki, T. ; Mouri, S. ; Tanaka, K. ; Ikemoto, Y. ; Moriwaki, T. ; Kimura, H. ; Juhasz, G.

(Citation)

Physical Review B, 72(7):73108-73108

(Issue Date)

2005-08

(Resource Type)

journal article

(Version)

Version of Record

(URL)

<https://hdl.handle.net/20.500.14094/90000408>



Photoinduced spin crossover in a Fe-picolylamine complex: A far-infrared study on single crystals

H. Okamura,* M. Matsubara, and T. Nanba

*Graduate School of Science and Technology, Kobe University, Kobe 657-8501, Japan*T. Tayagaki,[†] S. Mouri, and K. Tanaka*Department of Physics, Graduate School of Science, Kyoto University, Kyoto 606-8502, Japan*

Y. Ikemoto, T. Moriwaki, and H. Kimura

*Japan Synchrotron Radiation Research Institute and SPring-8, Sayo 679-5198, Japan*G. Juhász[‡]*Department of Chemistry, Kyushu University, Fukuoka 812-8581, Japan*

(Received 12 May 2005; revised manuscript received 22 June 2005; published 23 August 2005)

Far-infrared spectroscopy has been performed on $[\text{Fe}(\text{2-picolylamine})_3]\text{Cl}_2\text{EtOH}$ (Fe-pic) single crystals to probe changes in the molecular vibrations upon the photoinduced and temperature-induced spin crossovers. Synchrotron radiation has been used as the far-infrared source to overcome the strong absorption and the small sizes of the samples. Absorption lines due to FeN_6 cluster vibrations, observed below 400 cm^{-1} , show strong intensity variations upon the crossover due to the compression/expansion of FeN_6 between high-spin and low-spin states. However, they remain almost unchanged between the photo- and temperature-induced high-spin states. This is in sharp contrast to the lines at $500\text{--}700\text{ cm}^{-1}$ due to intramolecular vibrations of the picolylamine ligands, which show marked variations between the two high-spin states. It is concluded that the most important microscopic difference between the two high-spin states arises from the ligands, which are likely to reflect different states of intermolecular bonding.

DOI: 10.1103/PhysRevB.72.073108

PACS number(s): 78.30.-j, 75.30.Wx

A photoinduced spin crossover observed in organometallic compounds, in which the spin state of transition-metal ions can be changed by a photoexcitation, has attracted much interest recently.¹ Fe(II)-based compound $[\text{Fe}(\text{2-pic})_3]\text{Cl}_2\text{EtOH}$ (2-pic: 2-picolylamine or 2-aminomethyl pyridine, EtOH: ethanol), referred to as the Fe-pic, has been well known as a prototypical compound showing photoinduced as well as temperature-induced spin crossovers.¹ As sketched in Fig. 1(a), an Fe^{2+} ion in Fe-pic is located in a nearly octahedral crystal field created by the three 2-pic ligands. Depending on the magnitude of the crystal-field splitting, Fe^{2+} takes either total spin $S=2$ (high spin) or $S=0$ (low spin), as sketched in Fig. 1(b). Well above $T_{1/2} \approx 118\text{ K}$, Fe-pic is in the high-spin state [high-temperature high-spin state (HTHS)]. Upon cooling through $T_{1/2}$, Fe-pic undergoes a crossover to the low-spin state [low-temperature low-spin state (LTLS)]. The width of the crossover is about 20 K, as observed by the change in the high-spin fraction, $\gamma_{\text{HS}}(T)$. The crossover is associated with an $\sim 8\%$ change in the average Fe-N distance, corresponding to the different crystal-field splittings in LTLS and HTHS. A photoinduced spin crossover from LTLS to a high-spin state can be caused by visible or near-infrared light irradiation. Below 40 K, this photoinduced high-spin state (PIHS) persists even after the excitation is turned off. The half-life in γ_{HS} reaches 160 min at 10 K.² Recently, it has been discovered that the development of PIHS in Fe-pic involves highly nonlinear responses to the photoexcitation, such as an incubation time, a threshold intensity, a steplike change in γ_{HS} with time, and a domain formation.³ These unique characteristics are not ex-

pected for a photoexcitation of isolated Fe^{2+} ions, and they strongly imply a cooperative interaction among the Fe^{2+} ions. It has been further suggested that the development of PIHS in Fe-pic should be a transition to a novel macroscopic phase under photoexcitation, referred to as the “*photoinduced phase transition*.”^{3,4}

To examine this suggestion, it is important to compare the microscopic nature of PIHS with that of HTHS. It was found^{6–8} that the Raman-infrared selection rules in Fe-pic were modified between HTHS and PIHS, which suggested a photoinduced symmetry lowering in PIHS. In contrast, detailed x-ray-diffraction (XRD) studies of Fe-pic⁹ under photoexcitation found no significant difference in the average crystal structure between HTHS and PIHS. In addition, x-ray-absorption fine structure (XAFS) of Fe-pic showed that the local coordinations of the neighboring ions around Fe^{2+} were very similar between HTHS and PIHS.¹⁰ Recently, a nuclear resonant inelastic scattering (NRIS) experiment was reported on ^{57}Fe -enriched Fe-pic.¹¹ This technique selec-

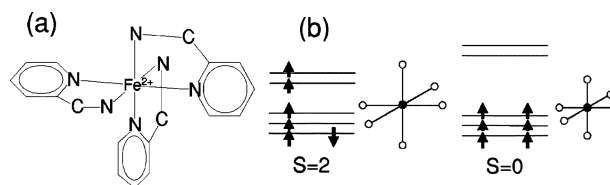


FIG. 1. (a) The structure of $[\text{Fe}(\text{2-pic})_3]^{2+}$. (b) Electron configurations of Fe^{2+} in high-spin ($S=2$) and low-spin ($S=0$) states. The average Fe-N bond length is larger in the $S=2$ state corresponding to the smaller crystal-field splitting.

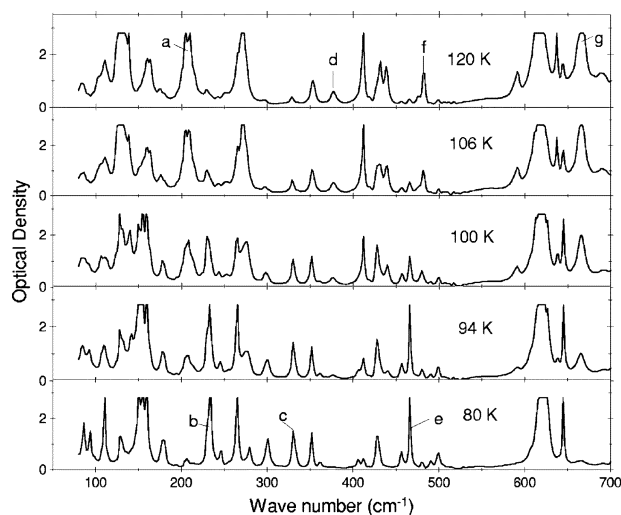


FIG. 2. Optical density of Fe-pic at several temperatures without photoexcitation. The labels a–g indicate the absorption bands and lines analyzed in Fig. 3.

tively probed the partial vibrational density of states for ^{57}Fe , which turned out to be very similar between LTLS and PIHS. Detailed XRD experiments at temperatures near $T_{1/2}$ (Ref. 12) and in the decay process after photoexcitation,¹³ and optical absorption experiments under photoexcitation, were also performed recently.¹⁴

In this work, we have measured the far-infrared (FIR) absorption spectra of Fe-pic single crystals in the 80–700 cm^{-1} range. Unlike the previous midinfrared work,⁸ this range can cover the normal-mode vibrations of the FeN_6 cluster. To analyze the observed data, the frequencies of molecular vibrations are also calculated for $[\text{Fe}(\text{2-pic})_3]^{2+}$ using the density-functional method. Many of the observed absorption lines below 400 cm^{-1} are attributed to the FeN_6 cluster vibrations, which exhibit characteristic intensity changes upon the photo- and temperature-induced spin crossovers. However, they are almost unchanged between HTHS and PIHS. It is concluded that the microscopic vibrational states of the FeN_6 cluster are similar between PIHS and HTHS, and that the deformation of 2-pic ligand should play an important role in the development of PIHS.

Powders of Fe-pic were synthesized from 2-pic, FeCl_2 , and ethanol, and then single crystals were obtained by recrystallization from their ethanol solution. Plate-shaped samples of approximately $0.7 \times 0.7 \times 0.1 \text{ mm}^3$ were obtained by cleaving the crystals, and mounted on a continuous-flow liquid He cryostat. The FIR absorption experiment was done using a synchrotron radiation (SR) source and a custom-made microscope at the beam line BL43IR, SPring-8.¹⁵ The SR source can deliver much higher photon flux density to the sample than the usual FIR sources. Since the Fe-pic single crystals had small sizes and strong FIR absorption, the use of SR was crucial to successfully perform this experiment. A black polyethylene filter was used to cut the visible component of the SR. Photoexcitation of the sample was made using white light from a tungsten lamp. A Si bolometer was used as a detector, and a Fourier-transform interferometer was used to record the spectra. The spectral resolution was set to 4 cm^{-1} .

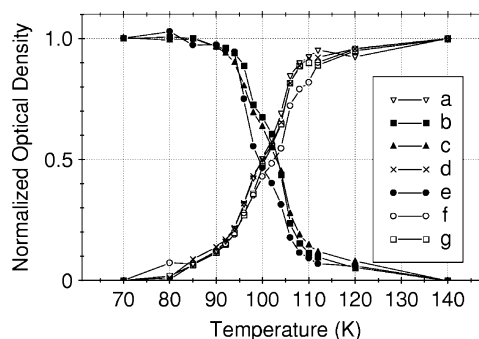


FIG. 3. Optical density (OD) of selected absorption lines and bands for Fe-pic, which are indicated in Fig. 2 by the labels a–f, as a function of temperature. The OD has been integrated over wave-number regions of (a) 187–224 cm^{-1} , (b) 224–241 cm^{-1} , (c) 322–340 cm^{-1} , (d) 365–392 cm^{-1} , (e) 462–471 cm^{-1} , (f) 473–488 cm^{-1} , and (g) 650–680 cm^{-1} , then normalized by the difference of OD between 70 and 140 K.

Figure 2(a) shows the FIR absorption spectra of Fe-pic without photoexcitation at several temperatures across $T_{1/2}$. Here, the absorption is expressed as the optical density (OD), $-\log[I(\nu)/I_0(\nu)]$, where $I(\nu)$ and $I_0(\nu)$ are the transmission spectra with and without the sample, respectively. The detection limit for the weak transmission was an OD of about 2.8 with an accumulation time of 2 min, and Fig. 2 shows the spectra below an OD of 2.8 only. The positions of the lines above 450 cm^{-1} agree well with those previously observed, which result from the intramolecular vibrations of the 2-pic ligand and ethanol.⁸ In contrast, many of the lines below 450 cm^{-1} are attributed to vibration modes of the FeN_6 cluster, as discussed later. The absorption lines show quite strong intensity variations through $T_{1/2}$. The detailed temperature dependence of several bands and lines, indicated by the labels in Fig. 2, is displayed in Fig. 3. It is seen that the variation of the absorption strength occurs over a temperature interval of about 20 K,¹⁶ which agrees well with that of γ_{HS} .⁸ Namely, the absorption strength closely reflects the evolution of the electronic configuration at Fe^{2+} and the associated deformation in the Fe-pic molecule upon the crossover.

Figures 4(a)–4(c) present the absorption spectra of Fe-pic in LTLS at 9 K, in PIHS at 9 K, and in HTHS at 140 K, respectively.¹⁷ Here, spectrum (a) was first recorded, then the sample was photoexcited with a 2 mW/mm^2 power density of white light for 5 min. After turning off the excitation, spectrum (b) was measured, then the sample was warmed up, and spectrum (c) was recorded. Upon the initial photoexcitation, the Fe^{2+} ions undergo d - d transitions to higher-lying states, then rapidly relax to the metastable PIHS.¹ The spectra above 450 cm^{-1} agree well with those reported previously:⁸ The double lines at 530–570 cm^{-1} , marked by the label δ , are observed in PIHS, but not in LTLS and HTHS.^{6,8} In addition, the lines in the 570–700 cm^{-1} range show marked differences between PIHS and HTHS, except for the line p_4 , which is due to C-H deformation mode of the 2-pic ligand.⁸ These lines have been attributed to skeletal vibrations of the aminomethyl group ($-\text{NH}-\text{CH}_2-$) in the 2-pic ligand.⁸ Hence the variations of these lines were re-

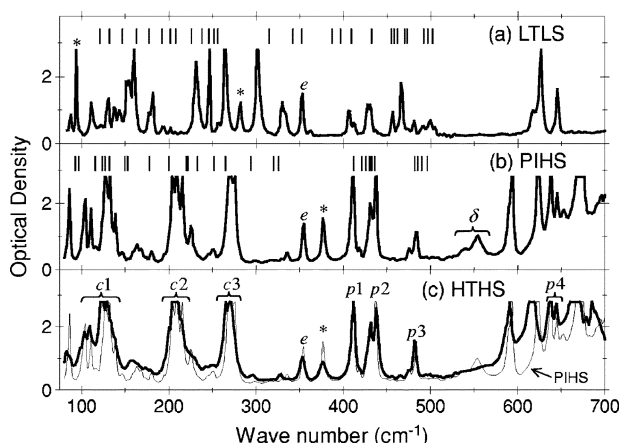


FIG. 4. Optical density spectra of Fe-pic in (a) LTLS at 9 K, (b) PIHS at 9 K, and (c) HTHS at 140 K. The thin curve in (c) is the same as the spectrum in (b), shown for comparison. The vertical bars in (a) and (b) show the calculated frequencies of molecular vibrations for $[\text{Fe}(\text{2-pic})_3]^{2+}$. See text for the labels.

garded as evidence for microscopic deformations in the 2-pic ligand between HTHS and PIHS.

To analyze the data below 450 cm^{-1} , we have calculated the frequencies of infrared-active molecular vibrations for an isolated $[\text{Fe}(\text{2-pic})_3]^{2+}$ using the density-functional method. The calculation was made using the GAUSSIAN '03 program,¹⁸ the details of which were similar to those previously reported.¹¹ The parameters involved in the calculation were first optimized so as to reproduce the reported molecular structure of $[\text{Fe}(\text{2-pic})_3]^{2+}$, then they were used to calculate the infrared frequencies. The calculated vibration frequencies are displayed by the vertical bars in Figs. 4(a) and 4(b). It is seen that most of the observed lines have their frequencies close to the calculated ones. (Note that line *e* should be due to ethanol or other modes related with intermolecular bonding, since it is hardly affected by the crossover.) The lines marked by the asterisks are located far apart from the calculated frequencies. This deviation should be related to the strong hydrogen bonding between the amine group ($-\text{NH}-$) of 2-pic and Cl^- ,⁵ which was neglected in the calculation. The calculated lines below 300 cm^{-1} in the high-spin states and those below 400 cm^{-1} in LTLS are mainly derived from the FeN_6 vibration modes. Hence the observed lines in these frequency ranges are also attributed to FeN_6 -based vibrations (except for line *e*). The lines *p1*–*p3* are attributed to intramolecular vibrations of 2-pic ligand (*p1* due to out-of-plane bending of the pyridine ring, *p2* and *p3* due to C-H deformation of the C-C portion).^{8,19}

In Fig. 4, the spectra below 300 cm^{-1} in PIHS and HTHS [(b) and (c)] are very similar to each other. They mainly consist of the three strong bands labeled as *c1*–*c3* in Fig. 4(c), which are due to stretching and deformation modes of the FeN_6 cluster. The spectral similarity demonstrates that the microscopic vibrational states of the FeN_6 cluster are also similar between PIHS and HTHS. In contrast, the spectrum in LTLS, Fig. 4(a), appears quite different from those of the high-spin states. The bands *c1*–*c3* are no longer observed in LTLS. Instead, a larger number of narrower lines are ob-

served, which may imply a symmetry lowering of FeN_6 in LTLS. However, the geometrical symmetry of the FeN_6 in the average crystal structure is nearly the same between the high- and low-spin states,^{5,9} hence the above spectral differences are more likely to result from changes in the force constants of Fe-N bonds. The occupation of t_{2g} orbitals by six electrons in LTLS, as sketched in Fig. 1(b), results in not only the shorter Fe-N distances, but also stronger Fe-N bonds.¹

The present data have demonstrated that the microscopic vibrational states of FeN_6 are very similar between PIHS and HTHS. This is consistent with the previous results of XRD,⁹ XAFS,¹⁰ and NRIS,¹¹ all of which gave very similar data between PIHS and HTHS. Compared with the previous works, however, it is very important that the present work has explicitly and directly shown the microscopic similarity with a high spectral resolution. In contrast, as already mentioned, the absorption spectrum at the $530\text{--}700\text{ cm}^{-1}$ range has shown clear differences between PIHS and HTHS, due to skeletal deformation of the 2-pic ligand.^{7,8} Considering these results, therefore, *the most important microscopic difference between the PIHS and HTHS of Fe-pic should be the deformation of 2-pic ligands*. Note that this deformation does not have a long-range order, since the XRD data⁹ show no appreciable deformation of 2-pic in the average crystal structure.

The unusual properties of PIHS, mentioned earlier, apparently result from a cooperative interaction (cooperativity) among Fe^{2+} ions. However, a cooperativity is very important also in the thermal spin crossover between HTHS and LTLS.¹ This was experimentally demonstrated on the diluted system (Fe, Zn)-pic, where the spin crossover became much broader at low Fe fractions, approaching that given by the Boltzmann distribution over isolated molecules.²⁰ An important source of cooperativity is the long-range elastic interaction, caused by the compression/expansion of FeN_6 upon the crossover.^{1,20,21} In this mechanism, an increase in the density of high-spin Fe^{2+} effectively increases the interaction (or equivalently lowers the energy difference between low- and high-spin states²²), accelerating the crossover compared with the isolated case.^{20,22} A theory based on the elastic interaction has also successfully reproduced two key properties of PIHS under photoexcitation,²² i.e., the presence of an incubation period and the threshold excitation intensity.³

In the above models, however, the microscopic properties involved in the interaction are not taken into account. In addition, short-range interaction among Fe^{2+} ions is neglected. It has been pointed out that the steplike change of γ_{HS} and the phase separation in PIHS cannot be understood without the short-range interaction.²² It is therefore important to characterize the interaction among Fe^{2+} ions more microscopically. As mentioned before, the $-\text{NH}-$ portion of the aminomethyl group in the 2-pic ligand is strongly hydrogen-bonded to the Cl^- anion. This hydrogen bonding is also responsible for the intermolecular bonding and crystallization of Fe-pic molecules.⁵ Hence, the microscopic deformation of 2-pic ligand found in the present work is quite likely to reflect different states of intermolecular bondings between HTHS and PIHS. To further characterize such bonding, it should be very useful to study the vibration modes below the

frequency range of this work. The intermolecular vibration modes, which involve the vibration of the entire $[\text{Fe}(\text{2-pic})_3]^{2+}$ ion, are expected to appear well below 80 cm^{-1} . Such modes are expected to be more sensitive to changes in the intermolecular bonding than those observed in this work.

Low-frequency vibrations may be important also in terms of the vibrational entropy.²³ For the thermal crossover in Fe-pic, the phonon contribution (ΔS_{ph}) of the experimentally observed entropy change was estimated to be as large as 56%.²⁴ This acts as a strong driving force for the crossover and also increases the cooperativity.^{1,25} The large ΔS_{ph} results from the strong anharmonicity of the FeN_6 vibrations: When the average lattice constants change upon the crossover, the phonon frequencies also change due to the anharmonicity. Consequently, the phonon density of states is modified, leading to the large ΔS_{ph} .^{23,24} Since the photoinduced crossover is observed at much lower temperatures, high-frequency phonons are quenched, and phonons with much lower frequencies may play important roles in terms of the entropy in PIHS. It is interesting that, in Fig. 4(c), the absorption band $c1$ shows significant broadening in HTHS compared to that in PIHS. This broadening of $c1$ seems unusually larger than

those of $c2$ and $c3$, compared with phonons in the usual solids having similar frequencies. This might be a sign of the strong anharmonicity of the low-frequency FeN_6 vibrations. Again, a further study at the lower-frequency range is needed to obtain more information about the role of phonon anharmonicity.

In conclusion, we have reported a FIR absorption study of Fe-pic single crystals in its three characteristic states. The absorption lines below 400 cm^{-1} are mainly attributed to the FeN_6 vibrations. The spectra are found very similar between PIHS and HTHS, which demonstrate that the microscopic environment at the FeN_6 cluster is also similar. The most important microscopic difference between HTHS and PIHS is the deformation of the 2-pic ligand, which should have important effects on the intermolecular coupling. The present result suggests the importance of further study at lower frequencies, which should give more insight into the microscopic nature of the intermolecular interaction in PIHS.

The experiments at SPring-8 were performed under the approval of JASRI (2004A0480-NSa-np).

*Email address: okamura@kobe-u.ac.jp

[†]Present address: SORST, Japan Science and Technology Corporation, Tokyo 113-8656, Japan.

[‡]Present address: Department of Chemistry, Carnegie Mellon University, Pittsburgh, PA 15213.

¹For a review, see, for example, P. Gülich, A. Hauser, and H. Spiering, *Angew. Chem., Int. Ed. Engl.* **33**, 2024 (1994); P. Gülich, Y. Garcia, and H. A. Goodwin, *Chem. Soc. Rev.* **29**, 419 (2000).

²H. Romstedt, A. Hauser, and H. Spiering, *J. Phys. Chem. Solids* **59**, 265 (1998).

³Y. Ogawa, S. Koshihara, K. Koshino, T. Ogawa, C. Urano, and H. Takagi, *Phys. Rev. Lett.* **84**, 3181 (2000).

⁴*Photoinduced Phase Transitions*, edited by K. Nasu (World Scientific, Singapore, 2004).

⁵M. Mikami, M. Konno, and Y. Saito, *Acta Crystallogr., Sect. B: Struct. Crystallogr. Cryst. Chem.* **36**, 275 (1980).

⁶T. Tayagaki and T. Tanaka, *Phys. Rev. Lett.* **86**, 2886 (2001).

⁷T. Tayagaki, K. Tanaka, and H. Okamura, *Phys. Rev. B* **69**, 064104 (2004).

⁸H. Okamura, M. Matsubara, T. Tayagaki, K. Tanaka, Y. Ikemoto, H. Kimura, T. Moriwaki, and T. Nanba, *J. Phys. Soc. Jpn.* **73**, 1355 (2004).

⁹N. Huby, L. Guerin, E. Collet, L. Toupet, J.-C. Ameline, H. Cailleau, T. Roisnel, T. Tayagaki, and K. Tanaka, *Phys. Rev. B* **69**, 020101(R) (2004).

¹⁰H. Oyanagi, T. Tayagaki, and K. Tanaka, in *X-Ray and Inner-Shell Processes*, edited by A. Marcelli *et al.*, AIP Conf. Proc. No. 652 (AIP, New York, 2003), p. 438.

¹¹G. Juhász, M. Seto, Y. Yoda, S. Hayami, and Y. Maeda, *Chem. Commun. (Cambridge)* **2004**, 2574 (2004).

¹²D. Chernyshov, M. Hostettler, K. W. Törnroos, and H.-B. Bürgi, *Angew. Chem., Int. Ed.* **42**, 3825 (2003).

¹³J. Kusz, D. Schollmeyer, H. Spiering, and P. Gülich, *J. Appl. Crystallogr.* **38**, 528 (2005).

Crystallogr. **38**, 528 (2005).

¹⁴C. Enachescu, U. Oetliker, and A. Hauser, *J. Phys. Chem. B* **106**, 9540 (2002).

¹⁵Y. Ikemoto, T. Moriwaki, T. Hirono, S. Kimura, K. Shinoda, M. Matsunami, N. Nagai, T. Nanba, K. Kobayashi, and H. Kimura, *Infrared Phys. Technol.* **45**, 369 (2004).

¹⁶The curves in Fig. 3 show the midpoint of the crossover around 103 K, which is lower than $T_{1/2}$. This difference is due to a low thermal contact of the sample with the cryostat, which resulted from our effort of not rigidly mounting the sample to avoid causing an internal strain. At lower temperatures, the thermal conductivity of the sample becomes much higher, and the difference between the measured and actual temperatures should be smaller. Our discussions below will not be affected by such a temperature difference.

¹⁷Due to technical restrictions, the data in Fig. 3 were measured on a different sample from that for the data in Fig. 2. The former was slightly thicker, resulting in the stronger absorption in Fig. 3.

¹⁸M. J. Frisch, *Gaussian '03, Revision B.04* (Gaussian Inc., Pittsburgh, 2003).

¹⁹G. Socrates, *Infrared Characteristic Group Frequencies* (Wiley, New York, 1980).

²⁰H. Spiering, E. Meissner, H. Koppen, E. W. Müller, and P. Gülich, *Chem. Phys.* **68**, 65 (1982).

²¹N. Willenbacher and H. Spiering, *J. Phys. C* **21**, 1423 (1988).

²²K. Koshino and T. Ogawa, *J. Phys. Soc. Jpn.* **68**, 2164 (1999).

²³A. Bousseksou, J. J. McGarvey, F. Varret, J. A. Real, J.-P. Tuchagues, A. C. Dennis, and M. L. Boillot, *Chem. Phys. Lett.* **318**, 409 (2000).

²⁴K. Kaji and M. Sorai, *Thermochim. Acta* **15**, 185 (1985).

²⁵A. Bousseksou, H. Constant-Machado, and F. Varret, *J. Phys. I* **5**, 747 (1995).